Modified Bilateral Filter for the Restoration of Noisy Color Images

Conference Paper · September 2012

DOI: 10.1007/978-3-642-33140-4_7

2 authors:

Krystyna Malik

7 PUBLICATIONS **79** CITATIONS

SEE PROFILE

Bogdan Smolka

Silesian University of Technology

269 PUBLICATIONS **2,912** CITATIONS

SEE PROFILE

Modified Bilateral Filter for the Restoration of Noisy Color Images

Krystyna Malik and Bogdan Smolka

Silesian University of Technology, Department of Automatic Control,
Akademicka 16 Str, 44-100 Gliwice, Poland
krystyna.malik@polsl.pl, smolka@ieee.org

Abstract. In the paper a novel technique of noise removal in color images is presented. The proposed filter design is a modification of the bilateral denosing scheme, which considers the similarity of color pixels and their spatial distance. However, instead of direct calculation of the dissimilarity measure, the cost of a connection through a digital path joining the central pixel of the filtering window and its neighbors is determined. The filter output, like in the standard bilateral filter, is calculated as a weighted average of the pixels which are in the neighborhood relation with the center of the filtering window, and the weights are functions of the minimal connection costs. Experimental results prove that the new denoising method yields significantly better results than the bilateral filter in case of color images contaminated by strong mixed Gaussian and impulsive noise.

1 Introduction

Visual information processing is increasingly becoming widespread as multimedia becomes common in everyday life. With the expanding use of color images in various multimedia applications and the proliferation of color capturing and display units, the interest in color image enhancement is rapidly growing.

Quite often color images are corrupted by various types of noise introduced by malfunctioning sensors in the image formation pipeline, electronic instability of the image signal, faulty memory locations in hardware, aging of the storage material, transmission errors and electromagnetic interferences due to natural or man-made sources [1–4]. Therefore, noise reduction is one of the most frequently performed image processing operation, as the enhancement of images or video streams degraded by noise is indispensable to facilitate subsequent image processing steps.

In this work, we focus on the restoration of color images corrupted by mixed Gaussian and impulsive noise. The reduction of such kind of noise is quite a challenging task, as the techniques capable of reducing efficiently the Gaussian noise, fail in the presence of impulses and the methods suited for the removal of impulsive noise are mostly ineffective when restoring images distorted by other noise types [5–10].

J. Blanc-Talon et al. (Eds.): ACIVS 2012, LNCS 7517, pp. 72–83, 2012.

The most widely used filtering designs are based on the concept of the *Vector Median Filter* (VMF), whose output is computed using the concept of *vector ordering* of a set of pixels from the filtering window. The vector ordering scheme is defined through the sorting of the cumulated distances from a given pixel to all other pixels from the filtering window. Then the scalar sum of distances are sorted and the associated vectors can be correspondingly ordered [1,11,12]. The vector median filter is very effective at reducing impulsive noise, however its efficiency is decreased when the image is distorted by Gaussian noise and therefore in such a case the VMF is usually combined with other filtering solutions.

Many noise reducing designs are based on the concept of adaptive weighted averaging, where the weights are assigned to pixels from a filtering window according to some rules which downweight the influence of outliers [13–19].

An efficient scheme proposed in [20,21] divides the pixels of the filtering window into two sets. The first one consists of the pixels similar to the central pixel of the local window and the other one is composed of those pixels, which diverge greatly from the central pixel. The output is computed as a weighted average of the peer-group members.

Similar concept is utilized by the technique proposed in [22], which calculates the distances between the central pixel in a local window and its neighbors. If the number of pixels classified as close to the central pixel is higher than a predefined threshold then the pixel is treated as uncorrupted, otherwise it is replaced by a vector median of all pixels from W or an average of the uncorrupted pixels in W. In [23] the peer-group members were found using a technique based on the evaluation of the statistical properties of a sorted sequence of accumulated distances used for the calculation of the vector median. The peer-group concept has been also successfully extended to the fuzzy context, so that the proposed technique is able to remove mixed noise by combining a statistical method for impulse noise detection and a replacement scheme utilizing an averaging operation aimed at smoothing out the Gaussian noise component [24,25].

An efficient method of image denoising called *Non-Local Means* (NLM) was proposed in [26,27]. This method is based on a non-local averaging of the image pixels in such a way that the new pixel value of the restored image is estimated as a weighted average of the pixels, whose local neighborhood is similar to the local neighborhood of the pixel which is currently being processed. The NLM filter is extremely efficient when restoring images corrupted by Gaussian noise, but fails in the presence of distortions introduced by impulsive noise.

2 Bilateral Filter

Another powerful nonlinear noise reducing filtering design, whose aim is to smooth images while preserving their edges, called *Bilateral Filter* (BF) was proposed in [28] and discussed in [29–32].

In this method, the intensity value at each image pixel is being replaced by a weighted average of the grayscale values of pixels belonging to the local neighborhood. The weight function depends on the spatial distance between the

central pixel of the local filtering window and the neighboring pixels as well as on the difference of their intensities. The bilateral filter output $J(\boldsymbol{x})$ at image domain location $\boldsymbol{x}$ is defined as

$$J(\boldsymbol{x}) = \frac{1}{Z} \sum_{\boldsymbol{y} \in \mathcal{N}_{\boldsymbol{x}}} w(\boldsymbol{x}, \boldsymbol{y}) \cdot I(\boldsymbol{y}), \quad Z = \sum_{\boldsymbol{y} \in \mathcal{N}_{\boldsymbol{x}}} w(\boldsymbol{x}, \boldsymbol{y}), \tag{1}$$

where $\mathcal{N}_{\boldsymbol{x}}$ is the local neighborhood of $\boldsymbol{x}$ and $w(\boldsymbol{x}, \boldsymbol{y})$ is the weight assigned to pixel at location $\boldsymbol{y}$ which belongs to $\mathcal{N}_{\boldsymbol{x}}$. The weight assigned to pixel at $\boldsymbol{y} \in \mathcal{N}_{\boldsymbol{x}}$ is defined as

$$w(\boldsymbol{x}, \boldsymbol{y}) = w_S(\boldsymbol{x}, \boldsymbol{y}) \cdot w_I(\boldsymbol{x}, \boldsymbol{y}). \tag{2}$$

This weight is a result of multiplication of two components

$$w_S(\boldsymbol{x}, \boldsymbol{y}) = \exp\left(-\frac{\|\boldsymbol{x} - \boldsymbol{y}\|^2}{2\sigma_S^2}\right), \quad w_I(\boldsymbol{x}, \boldsymbol{y}) = \exp\left(-\frac{|I(\boldsymbol{x}) - I(\boldsymbol{y})|^2}{2\sigma_I^2}\right), \tag{3}$$

where $\|\cdot\|$ denotes the Euclidean distance between $\boldsymbol{x}$ and $\boldsymbol{y}$, σ_S and σ_I are weighting parameters in the *spatial* and *intensity* domains respectively.

The w_S weighting function decreases with the spatial distance and the pixels which are far away from the center of the processing window has low influence on the weighted average expressed by (1). The w_I weighting function is a decreasing function of the absolute difference of pixel intensities. Thus, the weight w_I operating in the intensity domain reduces the influence of pixels with significantly different intensities, which ensures the preservation of sharp image edges.

Figure 1 explains the construction of the bilateral filter. It depicts an exemplary filtering window (a), the array of Euclidean distances (b) between the central pixel and all other pixels of the window and the array of the absolute differences of intensities (c).

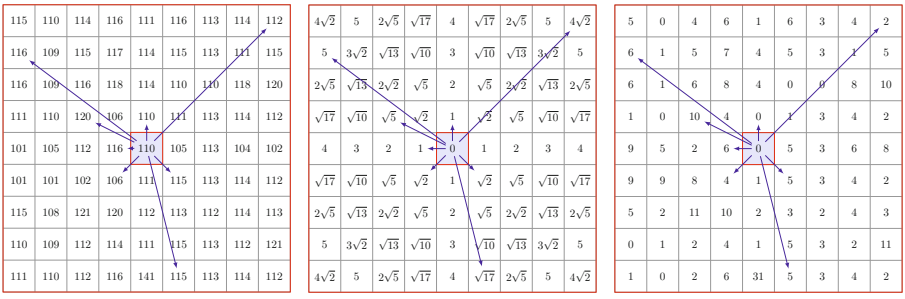

(a) filtering window (b) spatial distances (c) intensity differences

Fig. 1. Illustration of the bilateral filter construction

For color images, the difference of the intensity is replaced by the distance between color pixels in the RGB color space

$$\|\boldsymbol{I}(\boldsymbol{x}) - \boldsymbol{I}(\boldsymbol{y})\|^2 = \sum\nolimits_{k=1}^{3} \left(I_k\left(\boldsymbol{x}\right) - I_k\left(\boldsymbol{y}\right)\right)^2, \tag{4}$$

where $\|\boldsymbol{I}(\boldsymbol{x}) - \boldsymbol{I}(\boldsymbol{y})\|$ is the Euclidean distance between the color pixels $\boldsymbol{I}(\boldsymbol{x})$ and $\boldsymbol{I}(\boldsymbol{y})$ and the index represents the k-th color channel (Red, Green or Blue). Therefore, for color images the scheme given in (3) can be modified and the weight w_I can be expressed as

$$w_I(\boldsymbol{x}, \boldsymbol{y}) = \exp\left(-\frac{\|\boldsymbol{I}(\boldsymbol{x}) - \boldsymbol{I}(\boldsymbol{y})\|^2}{2\sigma_I^2}\right). \tag{5}$$

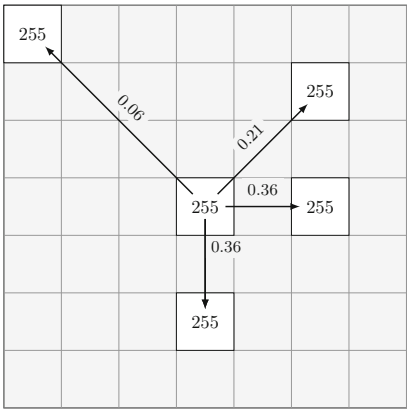

Fig. 2. Illustration of the BF inability to suppress impulsive noise

The bilateral filter is a highly efficient noise reducing scheme, however it has severe problems to remove the pixels introduced by impulsive noise process. Assuming that the central pixel of the local filtering window is an impulse and some of the pixels in the window are also injected by the noise and possess similar intensities or colors as the central pixel, then the weights expressed by (5) are relatively high, which leads to the preservation of the corrupted pixel.

This undesired effect is illustrated by the situation depicted in Fig. 2. The filtering window contains pixels whose intensities are equal to 128 and some white impulses. The weights assigned to gray pixels are very close to 0 for $\sigma_I = 20$, $\sigma_S = 2$ and the weights assigned to white pixels are depicted near the arrows. As a result the white impulse in the center of the filtering window will be preserved.

So, if in the close neighborhood of a noisy central pixel, another similar pixels corrupted by noise are present, then while calculating the new pixel value, the noisy pixel will be included with large weights and as a result the impulses will be preserved. Therefore, in this paper we propose a modification of the bilateral filter, which alleviates the described above drawback.

3 Modified Bilateral Filter

The concept of the proposed modification of the bilateral filter is based on assigning the pixels from the filtering window W a minimum connection cost of a digital path which joins them with the central pixel. In this way, each pixel is connected with the central pixel through a digital path with minimum cost function value. The cost of a connection is used to calculate a weight assigned to each pixel from W and the filter output is the weighted average of the local neighborhood.

For the calculation of the weights we treat the image as a graph and utilize the Dijkstra algorithm for finding the optimal connections between the pixels (graph vertices), where the graph weights are simply the absolute differences between adjacent pixels intensities. Thus, a connection cost of a pixel at position $\boldsymbol{y}$ is defined as a minimum sum of absolute differences between the pixels constituting a digital path connecting this pixel with the central pixel $I(\boldsymbol{x})$ [33].

For the computation of the optimal paths connecting the pixels with the central pixel $\boldsymbol{x}$ a cost array C is created. Initially $C(\boldsymbol{x}) = 0$ and $C(\boldsymbol{y}) = \infty$ for all other pixels $\boldsymbol{y}$ belonging to W, which indicates that the pixels were not yet assigned a connection cost value. At the beginning the cost of the crossing between the central pixel and its neighbors is calculated. Afterwards the Dijkstra algorithm assigns to each pixel in the window the lowest connection cost relative to the central pixel and creates the paths of the lowest total cost. Every pixel of W is visited and whenever a path with a lower cost is found, the current value in the array C is updated. Finally, this array includes the lowest costs and enables to find optimal paths connecting a given pixel with the starting point as shown in Fig. 3.

The connection costs can be treated as similarity measures between the central pixel of W and the pixels of the local neighborhood and in this way the

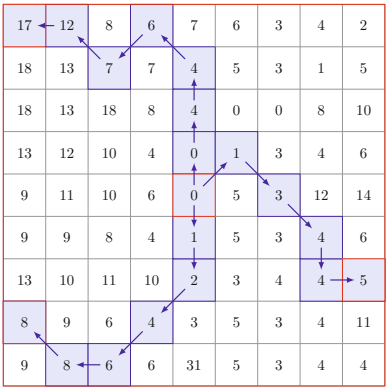

Fig. 3. Connection costs with some exemplary optimal paths

proposed filtering scheme is simply a weighted average of the pixels $\boldsymbol{y}$ which are in neighborhood relation with the central pixel $\boldsymbol{x}$. The weights are defined as

$$w(\boldsymbol{x}, \boldsymbol{y}) = \exp\left(-\frac{C(\boldsymbol{x}, \boldsymbol{y})^2}{h^2}\right), \tag{6}$$

where h is a tuning parameter and $C(\boldsymbol{x}, \boldsymbol{y})$ is a cost function of the optimal path connecting $\boldsymbol{x}$ and $\boldsymbol{y}$.

The cost function is the sum of the connection costs of the pixels creating the optimal optimal paths:

$$C(\boldsymbol{x}, \boldsymbol{y}) = \sum_{j=1}^{m} \left| I(\boldsymbol{x}_j) - I(\boldsymbol{x}_{j-1}) \right|, \tag{7}$$

where $\boldsymbol{x}_0 = \boldsymbol{x}$ is the starting point of a path, $\boldsymbol{x}_m = \boldsymbol{y}$ and m is the number of path segments.

For color images the connection costs are calculated using the Euclidean distance in RGB color space between neighboring pixels. Thus, the structure of filter output is the same as in the case of the bilateral filter

$$\boldsymbol{J}(\boldsymbol{x}) = \frac{1}{Z} \sum_{\boldsymbol{y} \in \mathcal{N}_{\boldsymbol{x}}} w(\boldsymbol{x}, \boldsymbol{y}) \cdot \boldsymbol{I}(\boldsymbol{y}), \quad Z = \sum_{\boldsymbol{y} \in \mathcal{N}_{\boldsymbol{x}}} w(\boldsymbol{x}, \boldsymbol{y}). \tag{8}$$

4 Experimental Results

In this section we compare the bilateral filter with the proposed modification in terms of the visual quality of the restored image and also in terms of objective quality measures.

First, the relationship between the control parameters of the filters and the noise level was analyzed. The effectiveness of the new filter was tested on the standard color test images LENA, PEPPERS and GOLDHILL corrupted with Gaussian and mixed Gaussian and impulse noise.

We used two kinds of impulsive noise. In the first model, which will be denoted by I, the noisy signal is modeled as $\boldsymbol{x}_i = \{x_{i1}, x_{i2}, x_{i3}\}$, with $x_{ik} = \rho$ with probability π, and o_{ik} with probability $1 - \pi$. The original, uncorrupted image pixel is denoted by $\boldsymbol{o}_i$ and the contamination component ρ is a random variable, which takes the value 0 or 255 with the same probability. In this noise model the contamination of the color image components is uncorrelated and the overall contamination rate is $p = 1 - (1 - \pi)^3$.

The second type of impulsive noise, called random-valued or uniform noise denoted as U is modeled as $\boldsymbol{x}_i = \boldsymbol{\rho}_i$ with probability p, and $\boldsymbol{o}_i$ with probability $1 - p$, where $\boldsymbol{\rho}_i$ is a noisy pixel with all channels corrupted by noise of uniform distribution in the range [0, 255]. In the first model the noise can corrupt one, two or all three channels. In the second model all channels are contaminated by random values within the range [0, 255].

The test images were contaminated by: Gaussian noise of $\sigma = 10$, $\sigma = 20$, $\sigma = 30$, and mixed Gaussian and impulsive noise of $\sigma = 10$ and $p = 0.1$, $\sigma = 20$ and $p = 0.2$, $\sigma = 30$ and $p = 0.3$, where p denotes the contamination probability.

The noise removal capabilities of the modified bilateral filter were extensively tested. To quantitatively evaluate the denoising methods we used the Peak Signal to Noise Ratio (PSNR) measure [2].

As can be derived from (3) the properties of the bilateral filter are controlled by the parameters σ_S and σ_I. Figure 4 shows the dependence of the PSNR on the σ_I and σ_S values for the noisy images restored by the bilateral filter.

The values of PSNR depend mainly on σ_I parameter, however σ_S has strong influence on the PSNR value in the range $[1, 3]$. Examining the plots, it can be observed that the optimal value of σ_S is relatively insensitive to noise level in the case of mixed noise but has to be tuned when restoring images polluted by Gaussian noise.

The color images contaminated by mixed Gaussian and impulsive noise were also restored by the modified bilateral filter. This filter was applied for different values of the parameters h in (6) and the dependence of PSNR measure on the parameter h is depicted in Fig. 5.

As can be observed, for test images contaminated by Gaussian noise of increasing intensity, the optimal results depend significantly on the tuning parameter h. Similarly, as in the case of the bilateral filter, the value of h increases with the

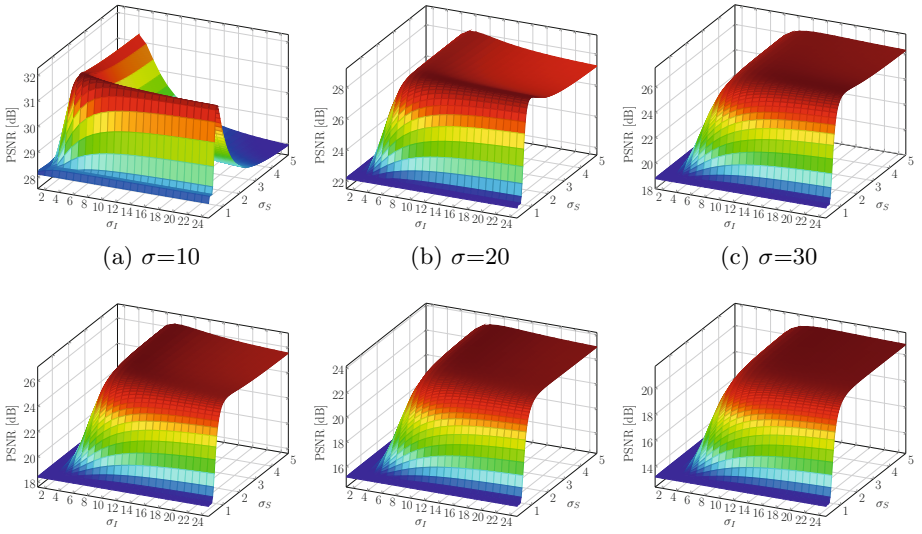

(a) σ=10 (b) σ=20 (c) σ=30

(d) σ=10, p=0.1 (e) σ=20, p=0.2 (f) σ=30, p=0.3

Fig. 4. Dependence of PSNR on σ_S and σ_I parameters for the bilateral filter operating in 5×5 window. The color image GOLDHILL was corrupted by Gaussian (a, b, c) and mixed Gaussian and impulsive, uniform noise U (d, e, f).

Table 1. Comparison of PSNR values obtained when restoring the color test images with the proposed algorithm and other denoising techniques

IMAGE	NOISE	FILTER								
		NLM	VMF	ANNMF	FVMF	VDF	$BF_{5\times5}$	$MBF_{5\times5}$	$BF_{9\times9}$	$MBF_{9\times9}$
LENA	$G(10)$	34.76	27.09	31.46	31.55	31.01	32.86	32.26	32.92	31.93
	$G(20)$	31.93	26.53	28.18	28.21	27.77	29.38	29.78	29.68	29.48
	$G(30)$	30.39	25.84	25.51	25.53	25.12	27.27	28.06	27.90	27.98
	$M(10)_I$	19.51	26.75	31.02	31.16	30.23	27.50	28.28	28.27	27.48
	$M(20)_I$	20.22	25.15	26.97	27.19	25.41	24.81	26.41	26.22	26.89
	$M(30)_I$	21.09	23.11	23.29	23.70	21.03	22.66	24.55	24.34	25.98
	$M(10)_U$	19.11	28.57	29.38	30.45	29.53	26.87	28.67	27.52	28.47
	$M(20)_U$	16.93	23.3	24.45	25.29	24.23	23.32	25.25	24.23	26.11
	$M(30)_U$	15.41	19.4	20.65	21.07	20.08	20.57	21.99	21.46	23.00
GOLDHILL	$G(10)$	33.40	25.31	29.47	29.55	28.71	31.90	30.91	31.90	30.74
	$G(20)$	30.21	24.94	27.04	27.11	26.18	28.56	28.30	28.74	27.98
	$G(30)$	28.19	24.47	24.74	24.85	23.70	26.47	26.79	26.84	26.55
	$M(10)_I$	17.92	25.00	29.13	29.11	23.24	25.52	25.99	26.16	25.13
	$M(20)_I$	19.68	23.92	25.81	26.11	20.36	23.91	24.95	25.06	25.15
	$M(30)_I$	20.63	22.29	21.61	22.93	17.31	21.97	23.50	23.51	24.70
	$M(10)_U$	19.34	27.25	27.98	28.70	27.84	26.33	27.32	26.7	26.94
	$M(20)_U$	17.53	22.89	23.44	24.67	22.92	23.36	24.84	24.08	25.33
	$M(30)_U$	15.48	19.42	19.69	21.03	19.02	20.93	22.16	21.74	22.98
PEPPERS	$G(10)$	33.71	26.54	30.85	31.13	30.32	32.15	31.74	32.29	31.55
	$G(20)$	31.31	25.97	27.86	28.07	27.23	28.73	29.51	28.92	29.39
	$G(30)$	29.81	25.27	25.23	25.47	24.55	26.70	27.61	27.13	27.75
	$M(10)_I$	18.54	26.01	30.27	30.66	29.22	26.37	26.95	27.07	26.46
	$M(20)_I$	19.48	24.50	26.11	26.86	24.17	23.46	24.87	24.69	25.61
	$M(30)_I$	19.68	22.96	21.84	23.29	19.56	21.18	22.82	22.57	24.37
	$M(10)_U$	18.49	28.13	28.47	29.91	28.33	26.04	27.96	26.68	28.02
	$M(20)_U$	16.62	22.93	23.20	24.84	23.16	22.35	24.24	23.14	25.18
	$M(30)_U$	14.36	19.05	19.35	20.66	19.07	19.61	21.03	20.36	21.98

noise magnitude. The obtained results also show that the optimal h parameter does not depend significantly on the image structure. For images contaminated by mixed Gaussian and impulse noise the optimal value of h is not considerably sensitive to the noise level. The range of of the h parameter, for which the optimal PSNR values can be obtained, is about $[200, 250]$.

The effectiveness of the new filtering design was compared with some of the existing methods:

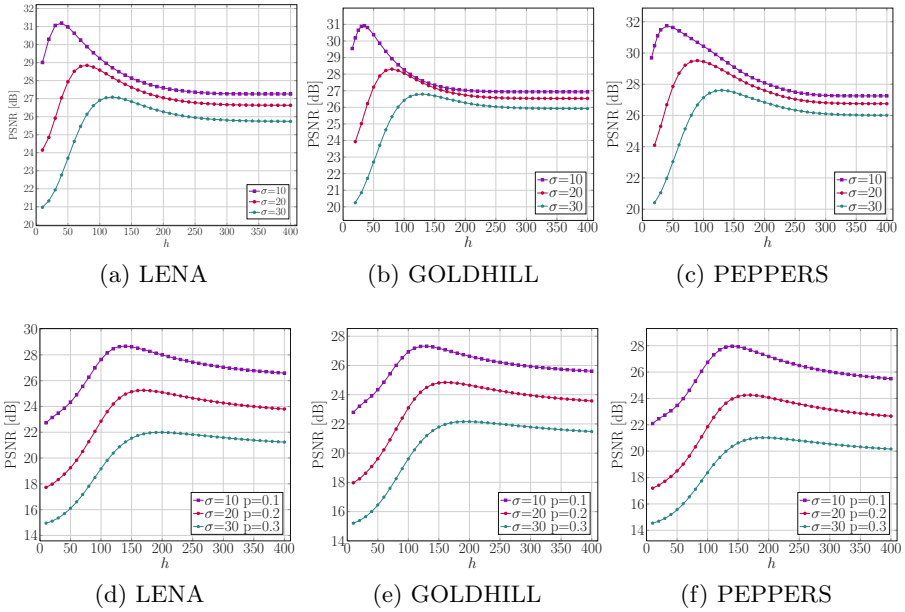

(a) LENA (b) GOLDHILL (c) PEPPERS

(d) LENA (e) GOLDHILL (f) PEPPERS

Fig. 5. Dependence of PSNR when applying the modified bilateral filter using a 5× 5 window on the h parameter for the color image PEPPERS corrupted with Gaussian (a, b, c) and mixed Gaussian and impulsive, uniform noise U (d, e, f)

- Non-Local Means filter (NLM) [26, 27],
- Vector Median Filter (VMF) [12],
- ANNMF - Adaptive Nearest-Neighbor Multichannel Filter [15],
- FVMF - Fuzzy Vector Median Filter [16–18],
- VDF - Vector Directional Filter [19] .

The *Bilateral Filter* (BF) and the proposed *Modified Bilateral Filter* (MBF) were tested for windows of size 5 × 5 and 9 × 9. The control parameters were selected experimentally to obtain optimal results in terms of the PSNR quality coefficient. The comparison of the efficiency of the proposed MBF with the mentioned above filters are summarized in Tab. 1.

As can be observed, for images contaminated by Gaussian noise, the best results are obtained by the NLM algorithm and the results of the modified bilateral are quite similar to those obtained using the bilateral filter. However, the results for images contaminated by mixed Gaussian and impulse noise obtained using the new filter are significantly better especially for images contaminated by high and medium mixed noise levels.

Figure 6 exhibits the restoration results of the modified and standard bilateral filter. As can be observed the image is smoothed, edges and details are better preserved and the filtering output is visually more pleasing. Unfortunately, as can be noticed in the images contaminated by a mixed Gaussian and impulse noise, small clusters consisting of two or more pixels distorted by impulsive

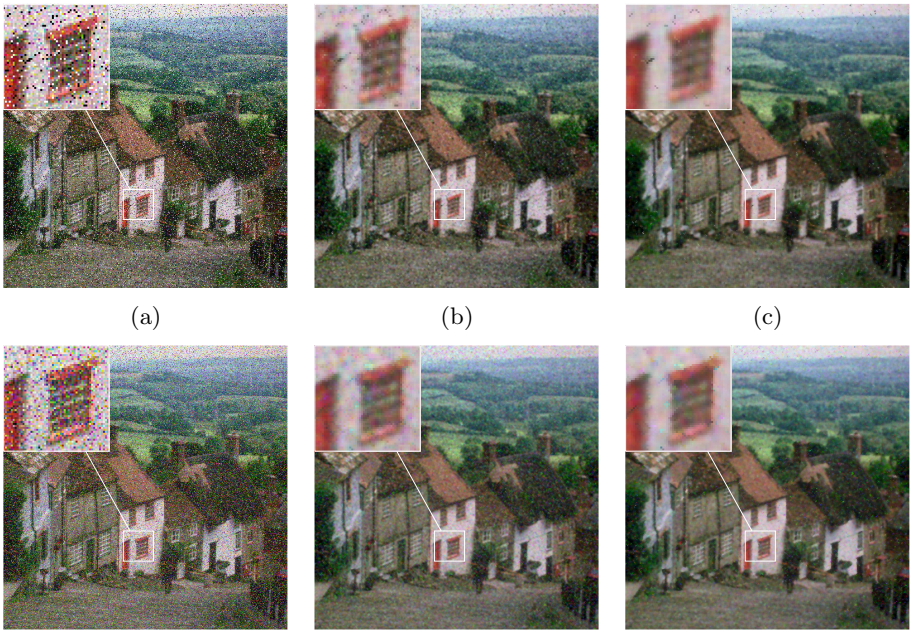

(a) (b) (c)

(d) (e) (f)

Fig. 6. Comparison of the efficiency of the bilateral filter with the proposed approach: (a) GOLDHILL image corrupted by mixed noise (σ=20, p=0.2, impulsive noise I), (b) BF output , (c) MBF output, (d) GOLDHILL image corrupted by mixed noise (σ=20, p=0.2, impulsive noise U), (e) BF output, (f) MBF output, (filtering window 5×5)

(a) PSNR=24.93 dB (b) PSNR=26.16 dB(c) PSNR=24.21 dB (d) PSNR=25.49 dB

Fig. 7. Results of the restoration of the test color image GOLDHILL corrupted by mixed noise (σ=20, p=0.2, impulsive noise U) using a 5×5 filtering window: (a) BF output , (b) MBF output, (c) BF with additional denoising of impulses using the method described in [22], (d) MBF with the same impulsive noise removal technique

noise are preserved. However, for images processed with the modified bilateral, this artifact can be easily removed using a switching filter with good impulse detection mechanism [9, 34].

For images processed with the standard bilateral filter, the removal of the remaining impulse noise is more difficult, because the impulses are blurred by the image restoration technique. The restoration results with additional impulsive noise reduction, using the method described in [22], are presented in Fig. 7.

5 Conclusions

In the paper a novel filtering scheme has been presented and analyzed. The results of the performed experiment indicate that very good restoration quality has been achieved for color images contaminated by strong mixed Gaussian and impulsive noise. The new filtering method yields significantly better results in comparison with other denoising methods both in terms of subjective quality and objective restoration measures. The beneficial feature of the proposed method is the removal of mixed noise with preservation of edges and image details.

References

1. Lukac, R., Smolka, B., Martin, K., Plataniotis, K., Venetsanopoulos, A.: Vector filtering for color imaging. IEEE Signal Processing Magazine 22(1), 74–86 (2005)
2. Plataniotis, K., Venetsanopoulos, A.: Color Image Processing and Applications. Springer (2000)
3. Boncelet, C.G.: Image noise models. In: Bovik, A. (ed.) Handbook of Image and Video Processing. Communications, Networking and Multimedia, pp. 397–410. Elsevier Academic Press (2005)
4. Zheng, J., Valavanis, K., Gauch, J.: Noise removal from color images. Journal of Intelligent and Robotic Systems 7(3), 257–285 (1993)
5. Peng, S., Lucke, L.: Multi-level adaptive fuzzy filter for mixed noise removal. In: IEEE International Symposium on Circuits and Systems, ISCAS 1995, vol. 2, pp. 1524–1527 (1995)
6. Wang, C., L.-F. Sun, Yang, B., Liu, Y.M., Yang, S.Q.: Video enhancement using adaptive spatio-temporal connective filter and piecewise mapping. EURASIP J. Adv. Sig. Proc (2008)
7. Garnett, R., Huegerich, T., Chui, C., Wenjie, H.: A universal noise removal algorithm with an impulse detector. IEEE Transactions on Image Processing 14(11), 1747–1754 (2005)
8. Tang, K., Astola, J., Neuvo, Y.: Nonlinear multivariate image filtering techniques. IEEE Transactions on Image Processing 4(6), 788–798 (1995)
9. Lukac, R.: Adaptive vector median filtering. Pattern Recognition Letters 24(12), 1889–1899 (2003)
10. Lukac, R., Smolka, B., Plataniotis, K., Venetsanopoulos, A.: Vector sigma filters for noise detection and removal in color images. Journal of Visual Communication and Image Representation 17(1), 1–26 (2006)
11. Pitas, I., Tsakalides, P.: Multivariate ordering in color image filtering. IEEE Trans. on Circuits and Systems for Video Technology 1(3), 247–259, 295-296 (1991)
12. Astola, J., Haavisto, P., Neuvo, Y.: Vector median filters. Proceedings of the IEEE 78(4), 678–689 (1990)
13. Plataniotis, K., Androutsos, D., Venetsanopoulos, A.: Multichannel filters for image processing. Signal Processing: Image Communication 9(2), 143–158 (1997)

14. Lukac, R., Plataniotis, K., Venetsanopoulos, A., Smolka, B.: A statistically-switched adaptive vector median filter. Journal of Intelligent and Robotic Systems 42(4), 361–391 (2005)
15. Plataniotis, K., Sri, V., Androutsos, D., Venetsanopoulos, A.: An adaptive nearest neighbor multichannel filter. IEEE Transactions on Circuits and Systems for Video Technology 6(6), 699–703 (1996)
16. Plataniotis, K.N., Androutsos, D., Venetsanopoulos, A.N.: Fuzzy adaptive filters for multichannel image processing. Signal Processing 55(1), 93–106 (1996)
17. Plataniotis, K., Androutsos, D., Venetsanopoulos, A.: Adaptive fuzzy systems for multichannel signal processing. Proceedings of the IEEE 87(9), 1601–1622 (1999)
18. Chatzis, V., Pitas, I.: Fuzzy scalar and vector median filters based on fuzzy distances. IEEE Transactions on Image Processing 8(5), 731–734 (1999)
19. Trahanias, P., Venetsanopoulos, A.: Vector directional filters-a new class of multichannel image processing filters. IEEE Transactions on Image Processing 2(4), 528–534 (1993)
20. Kenney, C., Deng, Y., Manjunath, B.S., Hewer, G.: Peer group image enhancement. IEEE Transactions on Image Processing 10(2), 326–334 (2001)
21. Deng, Y., Kenney, C., Moore, M., Manjunath, B.S.: Peer group filtering and perceptual color image quantization. In: Proceedings of the 1999 IEEE International Symposium on Circuits and Systems, ISCAS 1999, pp. 21–24 (1999)
22. Smolka, B., Chydzinski, A.: Fast detection and impulsive noise removal in color images. Real-Time Imaging 11(5-6), 389–402 (2005)
23. Smolka, B.: Peer group switching filter for impulse noise reduction in color images. Pattern Recognition Letters 31(6), 484–495 (2010)
24. Morillas, S., Gregori, V., Peris-Fajarnes, G., Sapena, A.: New adaptive vector filter using fuzzy metrics. Journal of Electronic Imaging 16(3), 033007 (2007)
25. Morillas, S., Gregori, V., Hervas, A.: Fuzzy peer groups for reducing mixed Gaussian-impulse noise from color images. IEEE Transactions on Image Processing 18(7), 1452–1466 (2009)
26. Buades, A., Coll, B., Morel, J.M.: A non-local algorithm for image denoising. In: IEEE Conf. on Computer Vision and Pattern Recognition, CVPR 2005, vol. 2, pp. 60–65. Washington, DC (2005)
27. Buades, A., Coll, B., Morel, J.M.: A review of image denoising algorithms, with a new one. Multiscale Modeling and Simulation 4(2) (2006)
28. Tomasi, C., Manduchi, R.: Bilateral filtering for gray and color images. In: Proceedings of the IEEE Int. Conf. on Computer Vision, pp. 839–846 (1998)
29. Paris, S., Durand, F.: A fast approximation of the bilateral filter using a signal processing approach. Int. J. Comput. Vision 81(1), 24–52 (2009)
30. Barash, D.: Bilateral Filtering and Anisotropic Diffusion: Towards a Unified Viewpoint. In: Kerckhove, M. (ed.) Scale-Space 2001. LNCS, vol. 2106, pp. 273–280. Springer, Heidelberg (2001)
31. Barash, D.: Fundamental relationship between bilateral filtering, adaptive smoothing, and the nonlinear diffusion equation. IEEE Transactions on Pattern Analysis and Machine Intelligence 24(6), 844–847 (2002)
32. Elad, M.: On the origin of the bilateral filter and ways to improve it. IEEE Transactions on Image Processing 11(10), 1141–1151 (2002)
33. Falcao, A., Stolfi, J., de Alencar Lotufo, R.: The image foresting transform: theory, algorithms, and applications. IEEE Transactions on Pattern Analysis and Machine Intelligence 26(1), 19–29
34. Smolka, B., Plataniotis, K.N., Chydzinski, A., Szczepanski, M., Venetsanopoulos, A.N., Wojciechowski, K.: Self-adaptive algorithm of impulsive noise reduction in color images. Pattern Recognition 35(8), 1771–1784 (2002)